Density Functional Study of the Ground and Excited State Potential Energy Surfaces of a Light-Driven Rotary Molecular Motor (3*R*,3′*R*)-(*P*,*P*)-*trans*-1,1′,2,2′,3,3′,4,4′-Octahydro-3,3′-dimethyl-4,4′-biphenanthrylidene†

Andranik Kazaryan and Michael Filatov*

Zernike Institute for Advanced Materials, University of Groningen, Nijenborgh 4, 9747 AG Groningen, The Netherlands

Received: March 17, 2009; Revised Manuscript Received: July 1, 2009

Potential energy surfaces of the ground and the first excited singlet states of the (3*R*,3′*R*)-(*P*,*P*)-*trans*-1,1′,2,2′,3,3′,4,4′-octahydro-3,3′-dimethyl-4,4′-biphenanthrylidene rotary molecular motor have been investigated along the central C_4═$C_{4'}$ double bond twisting mode starting from the (*P*,*P*)-*trans* and from the (*P*,*P*)-*cis* conformations occurring in the photoisomerization cycle of this compound. The potential energy profiles obtained with the help of the state average spin restricted ensemble-referenced Kohn−Sham (SA-REKS) method feature minima on the excited state surface, the positions of which are displaced with respect to the barriers on the ground state surface toward the isomerization products, the (*M*,*M*)-*cis* and the (*M*,*M*)-*trans* conformations, respectively. The origin of these minima is analyzed and explained. The results of the present study suggest that the experimentally observed unidirectionality of photoinduced rotation in the above compound can be corroborated by the obtained profiles of the ground and excited state potential energy surfaces.

1. Introduction

Light-driven rotary molecular motors based on helical overcrowded alkenes represent a new promising class of functional compounds. Optical control of the rotary motion in these compounds is achieved via the cis to trans isomerization of a carbon−carbon double bond, which allows for a 180° rotation of one part of the molecule (rotor) with respect to another (stator). One of the first synthetic compounds in this class is the (3*R*,3′*R*)-(*P*,*P*)-trans-1,1′,2,2′,3,3′,4,4′-octahydro-3,3′-dimethyl-4,4′-biphenanthrylidene (**1**), which contains two identical fragments connected by a central carbon−carbon double bond.[1,2] Unidirectional rotation around the central double bond is carried out in four steps (strokes): two photoisomerization steps interconnected by two thermal relaxation steps shown schematically in Figure 1. Fast light-induced isomerization (*P*,*P*)-*trans*-**1** to (*M*,*M*)-*cis*-**2**, in the first stroke, is followed, in the second stroke, by the thermal relaxation to a more stable (*P*,*P*)-*cis*-**2** isomer, which is photoisomerized, in the third stroke, to the (*M*,*M*)-*trans*-**1** and, in the fourth stroke, relaxes thermally to the starting conformation (*P*,*P*)-*trans*-**1**.[1,2] Experimental observations suggest the occurrence of a unidirectional rotation in this system whereby the direction of rotation is governed by the helicity, (*P*,*P*) or (*M*,*M*), and the configuration at the stereogenic centers, (3*R*,3′*R*) or (3*S*,3′*S*), around the central carbon−carbon double bond.[2]

The maximum rotation rate is restricted by the rate of the thermally controlled helicity inversion steps. A substantial progress in adjusting these energy barriers by various structural modifications has led to a noticeable increase in the rotation rate.[3−5] At the same time, the photoinduced steps remain less studied and possibilities for their modification/optimization are much less investigated. In a recent ultrafast optical study of a rotary molecular motor, a mechanism of the photoisomerization step schematically shown in Scheme 1 was suggested on the basis of experimental results.[6] In particular, it was hypothesized[6] that the landscape of the potential energy surface (PES) of the first excited singlet state S_1 along the twisting mode features a minimum the position of which is displaced with respect to the maximum on the ground S_0 PES toward the isomerized product. Thus, upon a photoexcitation, the molecule undergoes a very fast (ca. 2 ps) twisting motion, which ends up in a conformation matching the product of isomerization. The subsequent relaxation to the ground state PES (ca. 16 ps) brings the molecule to the final isomer.[6] Although within this essentially one-dimensional twisting model relaxation to the ground state and occurrence of the conical inresections cannot be described, an attractive feature of this model is that the preferred direction of rotation can be seen already at the photoisomerization stage as given by the slope of the potential energy surface of the excited state.[7]

SCHEME 1: Schematic Representation of the Mechanism of Trans−Cis Photoisomerization in a Rotary Molecular Motor Suggested in Ref 6 on the Basis of Ultrafast Optical Experiments[a]

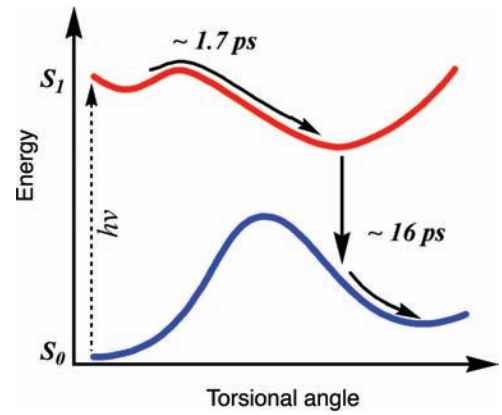

[a] The system resides in the excited state ca. 1.7 ps, after which it decays to the ground state during ca. 16 ps.

† Part of the "Walter Thiel Festschrift".

* Corresponding author. E-mail: m.filatov@rug.nl.

10.1021/jp902389j CCC: $40.75
Published on Web 07/23/2009

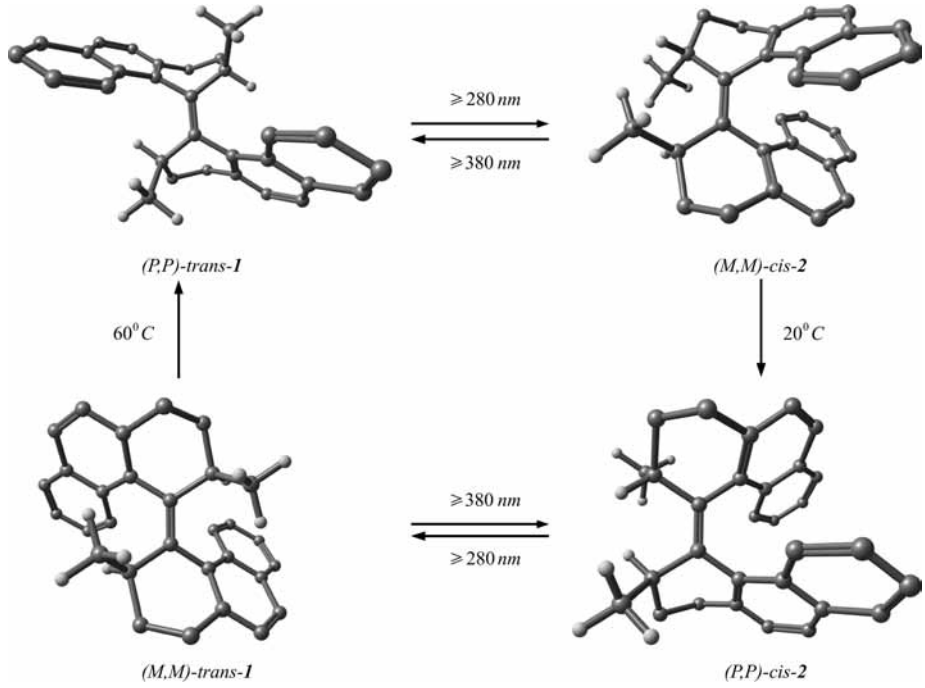

Figure 1. Four-stroke cycle of rotation in (3*R*,3′*R*)-(*P*,*P*)-*trans*-1,1′,2,2′,3,3′,4,4′-octahydro-3,3′-dimethyl-4,4′-biphenanthrylidene molecular motor.[1]

To verify this model, we undertake, in the present work, a first principles theoretical investigation of the potential energy surfaces of the ground and the lowest excited singlet states at the first and third (photoisomerization) steps in Figure 1. The major question addressed in this study is whether the potential landscapes of the ground and the first excited singlet states of the (3*R*,3′*R*)-(*P*,*P*)-*trans*-1,1′,2,2′,3,3′,4,4′-octahydro-3,3′-dimethyl-4,4′-biphenanthrylidene in different conformations can contribute to better understanding of unidirectionality of the rotation. Of course, complete modeling of the rotation process should include molecular dynamics simulations[7,10] and should address the problem of radiationless relaxation to the ground state. To approach the latter problem, one needs to analyze the nonadiabatic coupling vectors along possible trajectories on the excited state surface and to locate conical intersection points (seams) between the surfaces. The conical intersections are known to be very efficient funnels of radiationless relaxation processes.[11−13] However, to locate these points (or seams), one needs to go beyond the one-dimensional model and to take into account other degrees of freedom, such as a pyramidalization motion. An extended investigation of the potential energy surfaces that considers additional degrees of freedom and analysis of the nonadiabatic coupling vectors is currently in progress and will be reported elsewhere.

2. Method of Calculation

The potential energy surface of the ground and the first excited singlet states of compound **1** have been studied with the use of recently developed state-averaged (SA) variant of the spin restricted ensemble-referenced Kohn−Sham (REKS) method.[14] The minimal energy path (MEP) on the ground state potential energy surface (PES) along the $C_4{=}C_{4'}$ twisting mode (see Scheme 2) has been scanned with the use of the REKS method[15−19] for the (*P*,*P*)-*trans*-**1** to (*M*,*M*)-*cis*-**2** and for the (*P*,*P*)-*cis*-**2** to (*M*,*M*)-*trans*-**1** transitions. The B3LYP hybrid density functional[20] was employed in the PES scans.

Using the geometries obtained in the PES scan steps, the ground (S_0) and the first excited singlet (S_1) state energies have been calculated with the use of the SA-REKS method.[14] Along with the SA-REKS method, the time-dependent DFT (TD-DFT) formalism[21] has been used in the (S_0) and (S_1) PES calculations. The excited state calculations with both formalisms employed the BH&HLYP density functional.[22,23] Although the use of the BH&HLYP functional in the TD-DFT calculations leads to somewhat inferrior excitation energies than with the B3LYP functional,[24] this functional is employed in the present work because it provides a better compensation for the self-interaction error, which is important for the SA-REKS calculations.[14]

SCHEME 2: Numbering of Atoms in (3*R*,3′*R*)-(*P*,*P*)-*trans*-1,1′,2,2′,3,3′,4,4′-Octahydro-3,3′-dimethyl-4,4′-biphenanthrylidene

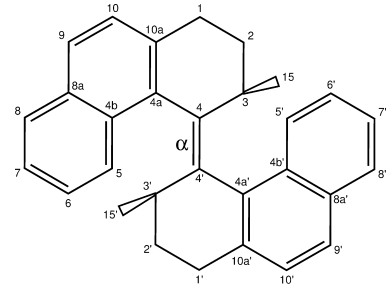

α=(4a, 4, 4',4a')

The basis set employed in the MEP scan was constructed from the standard 6-31G* basis set[25] on the central atoms and the STO-3G basis set[26] on the peripheral atoms. Stability of the so-obtained geometries with respect to basis set extension was checked at a number of points along the MEP by replacing this basis with the 6-31G* basis on all atoms. In the SA-REKS and TD-DFT calculations for the S_0 and S_1 PES, the 6-31G* basis set on all atoms was employed. At a number of selected points along the MEP, the calculations with the 6-311G** basis set[25] have been carried out to assess the significance of basis set effects.

TABLE 1: Vertical Excitation Energies in the (*P*,*P*)-*trans*-1 and (*P*,*P*)-*cis*-2 Conformations[a]

	SA-REKS		TDDFT	
	S_1-S_0	error	S_1-S_0	error
		(*P*,*P*)-*trans*-**1**		
1	4.87	0.81	4.79	0.73
2	4.47	0.41	4.27	0.21
3	4.41	0.35	4.19	0.14
exp[c]	4.06		4.06	
		(*P*,*P*)-*cis*-**2**		
1	4.65	0.44	4.63	0.42
2	4.23	0.02	4.17	−0.04
3	4.18	−0.03	4.10	−0.11
exp[c]	4.21		4.21	

[a] The excitation energies were calculated with the use of TD-BH&HLYP and SA-REBH&HLYP and three different basis sets.[b] Deviations from the experimental data are shown. All energies are in eV. [b] 1: hybrid 6-31G*/STO-3G. 2: 6-31G*. 3: 6-311G**. [c] Cited from ref 1.

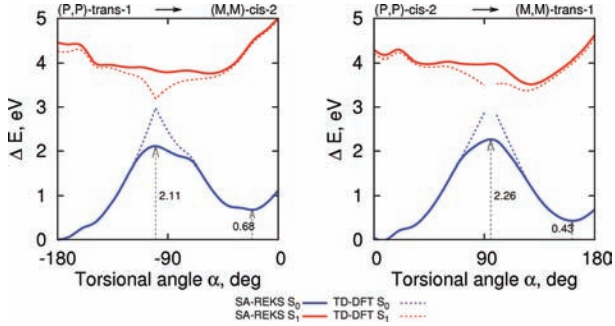

Figure 2. Profiles of the S_0 and S_1 PES for (*P*,*P*)-*trans*-**1** to (*M*,*M*)-*cis*-**2** (left panel) and (*P*,*P*)-*cis*-**2** to (*M*,*M*)-*trans*-**1** (right panel) photoisomerization steps along the C_4═$C_{4'}$ double bond twisting mode. The energies are given relative to the S_0 state energy of the most stable, (*P*,*P*)-*trans*-**1**, conformation at −180° of twist. The energy difference between (*P*,*P*)-*trans*-**1** and (*P*,*P*)-*cis*-**2** in the S_0 state is ca. 0.03 eV. See text for details of calculations.

3. Results and Discussion

The results of the calculations are collected in Table 1 and in Figure 2. More computational results can be found in the Supporting Information.[27] Figure 2 shows the profiles of the S_0 and S_1 PES along the MEP on the ground state surface. For both photoisomerization steps, (*P*,*P*)-*trans*-**1** to (*M*,*M*)-*cis*-**2** and (*P*,*P*)-*cis*-**2** to (*M*,*M*)-*trans*-**1**, the REKS method yields smooth PESs which feature potential energy barriers of 2.11 and 2.26 eV on the S_0 surfaces at the twisting angles near −100° and +95° of twist, respectively. These barriers originate from the avoided crossing between the diabatic $(...\pi^2)$ and $(...(\pi^*)^2)$ states which result from breaking of the C_4═$C_{4'}$ double bond near 90° of twist.[28,30] In a recent study, Torras et al.[29] with the help of the broken-symmetry spin-unrestricted B3LYP/6-31G* and MP2/6-31G* calculations have obtained somewhat lower energy barriers of 1.36 eV (BS-UB3LYP/6-31G*) and 1.41 eV (BS-UMP2/6-31G*) on the ground state PES of another synthetic molecular rotary motor, 9-(2,3-dihydro-2-phenyl-1*H*-benz[*e*]inden-1-ylidene)-9*H*-fluorene. The experimental estimates for the barrier heights are not available.

The S_1 PESs of the two steps feature minima at −56° (stroke 1) and 129° (stroke 3) of twist, which are displaced with respect to the maxima on the S_0 PESs toward the reaction products. Although the PESs plotted in Figure 2 were obtained with the use of the 6-31G* basis set, the extension to the 6-311G** basis set leads to rather modest variation (of ca. 0.05 eV) in the obtained excitation energies (see Table 1). The geometries obtained in the MEP scan with the combined 6-31G*/STO-3G basis do not substantially change upon replacement with the 6-31G* basis on all atoms. The use of the latter geometries optimized at a few points along the MEP leads to the energy variations in the subsequent SA-REKS calculations of the order of 0.01−0.03 eV.

The vertical excitation energies obtained with the use of the SA-REKS method and the 6-311G** basis set[25] for the (*P*,*P*)-*trans*-**1** (4.41 eV) and (P,P)-*cis*-**2** (4.18 eV) conformations are in a reasonable agreement with the available experimental data of 4.06 and 4.21 eV, respectively (see Table 1). It is noteworthy that the SA-REKS results (4.41 and 4.18 eV) are in a reasonably close agreement with the TD-DFT results for the two isomers, 4.19 and 4.10 eV, respectively. However, near the potential energy barrier on the ground state PES of both species, the single reference description employed in the TD-DFT formalism breaks down and the method cannot produce reliable excitation energies for these geometries.[14] This can be seen from the cusp on the S_0 PES and from the discontinuity of the S_1 PES as obtained in the TD-DFT calculations. However, near the energy minima on the ground state PES, where the single reference description is sufficiently adequate, the S_0 and the S_1 surfaces obtained in the SA-REKS and in the TD-DFT calculations are in good agreement with one another. The relative energies of the thermally unstable products of the photoisomerization steps, (*M*,*M*)-*cis*-**2** and (*M*,*M*)-*trans*-**1** with respect to the starting conformations (*P*,*P*)-*trans*-**1** and (*P*,*P*)-*cis*-**2** are predicted to be 0.68 and 0.43 eV, respectively, with the use of both SA-REKS and TD-DFT methods. This is in accord with the corresponding values reported previously by Feringa et al.:[5] 0.48 and 0.37 eV (AM1), and by Grimm et al.:[10] 0.52 and 0.37 eV (AM1); 0.58 and 0.41 eV (B3LYP/6-31G*), respectively.

The most striking feature of the obtained PESs of the ground and the first excited singlet states of the compounds **1** and **2** is the mismatch between the maxima on the S_0 PES and the minima on the S_1 PES. If one considers possible evolution of the molecular geometry of these species upon excitation, the most likely scenario is the relaxation of the geometry toward the minima on the excited state PES. The molecular geometry near these minima matches closely the geometry of the photoisomerization products, the (*M*,*M*)-*cis*-**2** and the (*M*,*M*)-*trans*-**1** species. This observation suggests that the relaxation to the ground S_0 state may proceed from a conformation which already matches the isomerization products. Therefore, the probability of falling back to the reactants should be rather small. Thus, the profile of the ground S_0 and the excited S_1 surfaces corroborates the observed unidirectionality of rotation in these species.[1,2,7−9]

Let us now turn to the electronic factors underlying the observed preference for the (*M*,*M*)-*cis*-**2** and the (*M*,*M*)-*trans*-**1** conformations on the excited state PES. Upon the photoexcitation of the reactants, (*P*,*P*)-*trans*-**1** and (*P*,*P*)-*cis*-**2**, the central C_4═$C_{4'}$ double bond is broken due to excitation of one electron from the π bonding to the π^* antibonding orbital of this bond. Therefore, the electronic structure of the excited S_1 state can be described as originating from a weak coupling between two substituted 1-methylnaphthyl radicals connected via a single C−C bond; see Scheme 3. In such a configuration, the π-conjugation between the C_4 and C_{4a} ($C_{4'}$ and $C_{4a'}$) is much stronger than in the ground state where the double C_4═$C_{4'}$ bond is relatively weakly conjugated with the naphthyl rings. Therefore, one can conjecture that, in the excited states, the

SCHEME 3: Schematic Representation of the Leading Lewis Structures of (3*R*,3′*R*)-(*P*,*P*)-*trans*-1,1′,2,2′,3,3′,4,4′-Octahydro-3,3′-dimethyl-4,4′-biphenanthrylidene in the Ground (Left Panel) and the Exited (Right Panel) States[a]

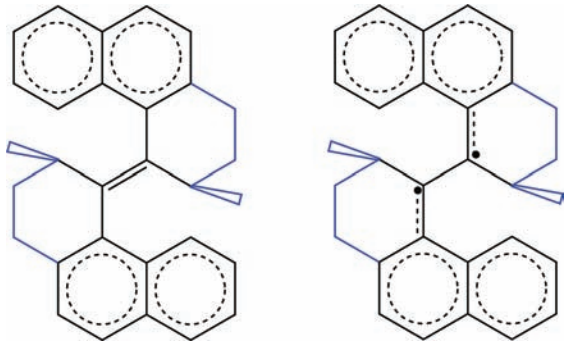

[a] The substituents to the 1-methylnaphthyl radicals are shown in blue.

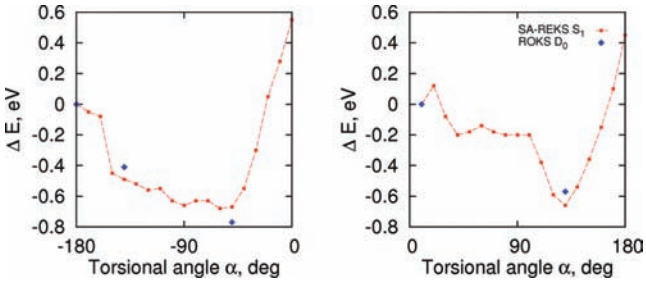

Figure 3. Energies of two substituted 1-methylnaphthyl radicals in comparison with the profiles of the excited state PES of both photoisomerization steps. The energies are given relative to the energy of the substituted 1-methylnaphthyl radical at −180° of twist (left panel) and at +10° of twist (right panel). See text for details of calculations.

deviation from the planarity of the 1-methylnaphthyl groups should result in a destabilization of the whole structure and vice versa.

To test this hypothesis, we have undertaken density functional calculations of the (appropriately substituted) 1-methylnaphthyl radical in the conformations taken from the geometries of the points on the MEP of **1** and **2** at −180°, −130°, −50°, +10°, and +130° of twist (see Figure 3). The relative energies (with respect to the −180° structure) of two isolated 1-methylnaphthyl radicals obtained from the ROKS/BH&HLYP/6-31G* calculations[31−34] in these conformations are shown in Figure 3 in comparison with the profiles of the excited state PESs for both photoisomerization steps. It is clearly seen that the minimum on the excited state PES originates due to the stabilization in the 1-methylnaphthyl radical units. Near the minima, the (*M*,*M*)-*cis*-**2** and the (*M*,*M*)-*trans*-**1** isomers adopt conformations in which the $C_{4b}-C_{4a}-C_4-C_{4'}$ ($C_{4b'}-C_{4a'}-C_{4'}-C_4$) dihedral angle is close to planarity thus providing better π-conjugation within the 1-methylnaphthyl radical units.

The ground state geometries of the (*M*,*M*)-*cis*-**2** and the (*M*,*M*)-*trans*-**1** conformations are strongly influenced by the steric repulsion between the lobes of the molecular rotor. The increased steric repulsion (as compared to the more stable (*P*,*P*)-*trans*-**1** and (*P*,*P*)-*cis*-**2** conformations) leads to an elongation of the central $C_4{=}C_{4'}$ double bond which then acquires some diradicaloid character. This, in turn, leads to a stronger π-conjugation between the C_4 and C_{4a} ($C_{4'}$ and $C_{4a'}$) atoms similar to that observed in the excited state. It is obvious, therefore, that the $C_{4b}-C_{4a}-C_4-C_{4'}$ ($C_{4b'}-C_{4a'}-C_{4'}-C_4$) dihedral angle in the ground state (*M*,*M*)-*cis*-**2** and (*M*,*M*)-*trans*-**1** conformations will be closer to planarity than in the more stable (*P*,*P*)-*trans*-**1** and (*P*,*P*)-*cis*-**2** conformations. This discussion implies that there is a correlation between the preference for the (*M*,*M*)-*cis*-**2** and the (*M*,*M*)-*trans*-**1** conformations on the excited state PES and their geometry near the corresponding minima on the ground state PES. Therefore, one can argue that the true energy minimum on the excited state PES of the above species can be found for the molecular geometry which strongly resembles the structure near the minimum on the ground state PES.

Although the profiles of the S_0 and S_1 PESs of **1** and **2** presented in Figure 2 may help one to explain the origin of the observed unidirectionality of rotation during the photoisomerization steps in Figure 1, the mechanism of relaxation to the ground state is not yet fully rationalized. The most likely scenario of the radiationless $S_0 \rightarrow S_1$ relaxation is that it proceeds via the nonadiabatic coupling to vibrational modes. Occurrence of the conical intersection (CI) points (or seams)[11−13] between the S_0 and S_1 surfaces near the minima on the excited state PESs of both species can indicate clearly the strength of nonadiabatic coupling in these regions. To find the CI points (see, e.g., ref 35 for a recent review on the search algorithms), one needs to go beyond the effectively one-dimensional model shown in Figure 2 and to consider motion of the lobes of molecular rotor along other degrees of freedom, such as the pyramidalization motion at the C_4 and $C_{4'}$ atoms. The search for the CI points is still in progress; however, the preliminary results obtained so far support the general picture outlined in this article.

4. Conclusions

In this work, we have undertaken a density functional study of the potential energy surfaces of the ground S_0 and the first excited singlet S_1 states of the (3*R*,3′*R*)-(*P*,*P*)-*trans*-1,1′,2,2′,3,3′,4,4′-octahydro-3,3′-dimethyl-4,4′-biphenanthrylidene (**1**) molecular motor. The S_1 excited state potential energy surfaces obtained in the SA-REKS calculations along the minimal energy path connecting the (P,P)-*trans*-**1** to (M,M)-*cis*-**2** conformations and the (P,P)-*cis*-**2** to (*M*,*M*)-*trans*-**1** conformations feature minima near the molecular geometries matching the isomerization products, (*M*,*M*)-*cis*-**2** and (*M*,*M*)-*trans*-**1**. Occurrence of the minima on the excited state PES is explained by the improved π-conjugation within the $C_4-C_{4a}-C_{4b}-C_{10a}$ ($C_{4'}-C_{4a'}-C_{4b'}-C_{10a'}$) fragments (see Schemes 2 and 3) in these conformations. The slope on the S_1 PESs of both conformations indicates that there is a preferred direction of rotation upon photoexcitation of the molecular motor. These theoretical findings are consistent with the conclusions made by Augulis et al.[6] on the basis of ultrafast optical experiments.

The results of the present study suggest that upon photoexcitation to the S_1 state, the molecular geometry of (*P*,*P*)-*trans*-**1** ((*P*,*P*)-*cis*-**2**) evolves quickly toward the isomerization product whereupon relaxation to the ground S_0 state occurs due to the nonadiabatic coupling with the vibrational modes. Although, in the present work, we do not report on the study of the radiationless relaxation process, the preliminary results obtained so far indicate that there is a conical intersection between the S_0 and S_1 PESs near the minimum on the S_1 surface. The presence of conical intersection points indicates a strong nonadiabatic coupling[12] in the regions adjacent to the minima on the S_1 PES. A detailed investigation of the dynamics of radiationless relaxation and a search for the conical intersection points (seams) are currently in progress. These results will be used for setting up molecular dynamics simulations of rotation cycle of the (3*R*,3′*R*)-(*P*,*P*)-*trans*-1,1′,2,2′,3,3′,4,4′-octahydro-3,3′-dimethyl-4,4′-biphenanthrylidene (**1**) molecular motor.

Supporting Information Available: Table of geometric parameters, table of vertical excitation energies, and atomic structure with bond numbering. This material is available free of charge via the Internet at http://pubs.acs.org.

References and Notes

(1) Harada, N.; Koumura, N.; Feringa, B. L. *J. Am. Chem. Soc.* **1997**, *119*, 7256.
(2) Koumura, N.; Zijlstra, R. W. J.; Delden, R. A.; Harada, N.; Feringa, B. L. *Nature* **1999**, *401*, 152.
(3) Pollard, M. M.; Meetsma, A.; Klok, M.; Pijper, D.; Feringa, B. L. *Adv. Funct. Mater.* **2007**, *17*, 718.
(4) Pollard, M. M.; Meetsma, A.; Feringa, B. L. *Org. Biomol. Chem.* **2008**, *6*, 507.
(5) Feringa, B. L.; Koumura, N.; van Delden, R. A.; ter Wiel, M. K. J. *Appl. Phys. A - Mater. Sci. Proc.* **2002**, *75*, 301.
(6) Augulis, R.; Klok, M.; Feringa, B. L.; Loosdrecht, P. H. M. *Phys. Status Solidi* **2009**, *6*, 181.
(7) Vacek, J.; Michl, J. *Adv. Funct. Mater.* **2007**, *17*, 730.
(8) Kottas, G. S.; Clarke, L. I.; Horinek, D.; Michl, J. *Chem. Rev.* **2005**, *105*, 1281.
(9) Albu, N. M.; Bergin, E.; David, J.; Yaron, D. J. *J. Phys. Chem. A* **2009**, *113*, 7090.
(10) Grimm, S.; Bruchle, C.; Frank, I. *ChemPhysChem* **2005**, *6*, 1943.
(11) Bernardi, F.; Olivucci, M.; Robb, M. A. *Chem. Soc. Rev.* **1996**, *25*, 321.
(12) Levine, B. G.; Martinez, T. J. *Annu. Rev. Phys. Chem.* **2007**, *58*, 613.
(13) Yarkony, D. R. *Rev. Mod. Phys.* **1996**, *68*, 985.
(14) Kazaryan, A.; Heuver, J.; Filatov, M. *J. Phys. Chem. A* **2008**, *112*, 12980.
(15) Filatov, M.; Shaik, S. *Chem. Phys. Lett.* **1999**, *304*, 429.
(16) Filatov, M.; Shaik, S. *J. Phys. Chem. A* **2000**, *104*, 6628.
(17) Cremer, D.; Filatov, M.; Polo, V.; Kraka, E.; Shaik, S. *Int. J. Mol. Sci.* **2002**, *3*, 604.
(18) Illas, F.; Moreira, I.; de, P. R.; Bofill, J. M.; Filatov, M. *Phys. Rev. B* **2004**, *70*, 132414.
(19) Illas, F.; Moreira, I.; de, P. R.; Bofill, J. M.; Filatov, M. *Theor. Chem. Acc.* **2006**, *116*, 587.
(20) Stephens, P. J.; Devlin, F. J.; Chabalowski, C. F.; Frisch, M. J. *J. Phys. Chem.* **1994**, *98*, 11623.
(21) Casida, M. In *Recent Advances in Density Functional Methods*; Chong, D. P., Ed.; World Scientific: Singapore, 1995; p 155.
(22) Becke, A. D. *J. Chem. Phys. Rev. Mod. Phys.* **1993**, *98*, 1372.
(23) Lee, C.; Yang, W.; Parr, R. G. *Phys. Rev. B* **1988**, *37*, 785.
(24) Silva-Junior, M. R.; Schreiber, M.; Sauer, S. P. A.; Thiel, W. *J. Chem. Phys.* **2008**, *129*, 104103.
(25) Krishnan, R.; Binkley, J. S.; Seeger, R.; Pople, J. A. *J. Chem. Phys.* **1980**, *72*, 650.
(26) Hehre, W. J.; Stewart, R. F.; Pople, J. A. *J. Chem. Phys.* **1969**, *51*, 2657.
(27) See the Supporting Information.
(28) Salem, L. *Science* **1976**, *191*, 822.
(29) Torras, J.; Rodriguez-Ropero, F.; Bertran, O.; Aleman, C. *J. Phys. Chem. C* **2009**, *113*, 3574.
(30) Salem, L.; Rowland, C. *Angew. Chem., Int. Ed. Engl.* **1972**, *11*, 92.
(31) Frank, I.; Hutter, J.; Marx, D.; Parinello, M. *J. Chem. Phys.* **1998**, *108*, 4060.
(32) Filatov, M.; Shaik, S. *Chem. Phys. Lett.* **1998**, *288*, 689.
(33) Filatov, M.; Shaik, S. *J. Chem. Phys.* **1999**, *110*, 116.
(34) Gräfenstein, J.; Kraka, E.; Cremer, D. *Chem. Phys. Lett.* **1998**, *288*, 593.
(35) Keal, T. W.; Koslowski, A.; Thiel, W. *Theor. Chem. Acc.* **2007**, *118*, 837.

JP902389J